Ion Binding Induces Closed Conformation in *Pseudomonas* 7A Glutaminase-Asparaginase (PGA): Crystal Structure of the PGA-SO_4^{2-}-NH_4^+ Complex at 1.7 Å Resolution[†,‡]

Clarissa G. Jakob,[§,||] Krzysztof Lewinski,[⊥] Michael W. LaCount,[§] Joseph Roberts,[▽] and Lukasz Lebioda*[,§]

Department of Chemistry and Biochemistry University of South Carolina, Columbia, South Carolina 29208, Department of Chemistry, Davidson College, Davidson, North Carolina 28036, Department of Chemistry, Jagiellonian University, 30-060 Cracow, Poland, and College of Pharmacy, University of South Carolina, Columbia, South Carolina 29208

Received August 7, 1996; Revised Manuscript Received October 11, 1996[⊗]

ABSTRACT: *Pseudomonas* 7A glutaminase−asparaginase (PGA) catalyzes the hydrolysis of D- and L-isomers of glutamine and asparagine. X-ray quality type-1 crystals of PGA have been obtained from 2.0 M ammonium sulfate. The space group is $C222_1$ with unit-cell dimensions $a = 78.62$, $b = 135.80$, and $c = 137.88$ Å. The tetrameric molecule is located on a crystallographic 2-fold axis, and two subunits form the asymmetric portion of the unit cell. The structure was solved by the molecular replacement method and refined at 1.7 Å resolution to an $R = 19.9\%$ with a good geometry of the model, $G = 0.05$. The resultant electron density maps enabled us to resolve individual constituent atoms of most residues and introduce minor revisions to the amino acid sequence. The catalytic loop, Thr20−Gly40, is in the closed conformation with excellent electron density in both subunits. A sulfate ion and an ammonium ion are bound in the substrate binding site and interact with the loop. This interaction appears to be responsible for the observed closed conformation. New arguments supporting Thr20 as the catalytic nucleophile in the asparaginase activity are proposed.

L-Asparaginases and L-glutaminases from a variety of bacterial sources have been shown to be effective chemotherapeutic agents for several neoplastic diseases. Treatment with these enzymes capitalizes on the lowered ability of cancerous cells to synthesize L-asparagine (Montgomery, 1976). This metabolic defect leads to a dependency for an exogenous supply of L-asparagine which is depleted by asparaginase treatment, thus effectively starving the cancer cells. *Escherichia coli* L-asparaginase (EcA)[1] has been used under the brand name Elspar as a treatment for acute lymphocytic leukemia for more than 20 years (Kidd, 1970). This enzyme is unfortunately not very effective in the treatment of solid tumors. However, the glutaminase−asparaginase isolated from *Pseudomonas* 7A (PGA) has shown significant anti-tumor activity in mice (Roberts et al., 1979) especially when combined with glutamine antimetabolites (McGregor & Robets, 1989). More recently, PGA has shown promise as a possible therapeutic agent for the treatment of retroviral diseases (Roberts & McGregor, 1991).

Glutaminase−asparaginase from *Pseudomonas* 7A (EC 3.5.1.38) belongs to a family of related amidohydrolases that catalyzes the deamidation of glutamine (Gln) and asparagine (Asn). The family of bacterial enzymes contains two classes of amidohydrolases. The first class includes asparaginases which are much more specific for Asn and catalyze the hydrolysis of asparagine to aspartic acid. The two best characterized enzymes that belong to this class are those isolated from *E. coli* (EcA) and from *Erwinia chrysanthemi* (ErA). The second class contains enzymes that are less specific and catalyze the hydrolysis of glutamine to glutamic acid and asparagine to aspartic acid with similar efficiency. The most studied representatives of this class are PGA and glutaminase−asparaginase from *Acinetobacter glutaminasificans* (AGA). The sequence and structural homology among both classes of enzymes are indicative of a common mechanism for deamidation (Swain et al., 1993; Miller et al., 1993; Lubkowski et al., 1994). Bacterial amidohydrolases are active as tetramers of identical subunits. Each subunit, with $M_r = 34-36$ kDa, contains an active site situated between adjacent monomers, but the four active sites per homotetramer do not possess functional cooperativity (Citri et al., 1972). Evidence for a double-displacement or "ping-pong" mechanism has been established (Röhm & Van Etten, 1986) making the amidohydrolases mechanistically similar to the thoroughly studied serine proteases, such as trypsin. The structural perspective on the enzymatic mechanism is primarily based on crystallographic studies compiled on EcA at 2.3 Å resolution (Swain et al., 1993) and ErA at 1.8 Å resolution (Miller et al., 1993). Lubkowski et al. (1994) determined the structure of PGA in the open conformation and reported that Thr100, Asp101, and Lys173 of PGA are the catalytic

[†] This research was supported in part by the National Science Foundation Grant MCB 901814.

[‡] The coordinates have been deposited with the Brookhaven Protein Data Bank (Accession Number 4pga).

* Corresponding author. Phone: 1 (803) 777-2140. FAX: 1 (803) 777-9521. E-mail: lebioda@psc.sc.edu.

[§] Department of Chemistry and Biochemistry, University of South Carolina.

[||] Davidson College.

[⊥] Jagiellonian University.

[▽] College of Pharmacy, University of South Carolina.

[⊗] Abstract published in *Advance ACS Abstracts,* January 1, 1997.

[1] Abbreviations: PGA, *Pseudomonas* 7A glutaminase−asparaginase; EcA, *Escherichia coli* L-asparaginase; ErA, *Erwinia chrysanthemi* L-asparaginase; AGA, *Acinetobacter glutaminasificans* glutaminase−asparaginase; MPD, 2-methyl-2,4-pentanediol.

S0006-2960(96)01979-4 CCC: $14.00

Table 1: Intensity Statistics of the X-ray Data Set

		shell (Å)										
	total	39.31−3.80	−3.02	−2.64	−2.40	−2.22	−2.09	−1.99	−1.90	−1.83	−1.77	−1.71
total no. of observations	178566	21452	20949	20701	19904	20227	18055	15677	14529	10989	8550	7533
no. of independent reflections												
theoretical	79799	7587	7279	7249	7161	7597	7180	6905	7470	6840	6790	7741
observed	68971	7353	7077	6936	6795	7080	6580	6124	6201	5313	4755	4757
average intensity (F^2/σ)		19.91	15.53	9.96	7.44	6.06	4.66	3.88	3.18	2.70	2.32	2.08
R_{merge}	7.5	4.7	6.0	9.0	11.9	14.3	18.0	20.1	23.4	25.0	25.8	26.1

residues on the basis of structural and sequence homology to EcA and ErA.

The precise catalytic mechanism for PGA and related amidohydrolases is still somewhat ambiguous. It tentatively proceeds via a double-displacement reaction. Initial nucleophilic attack on the amide carbon of Gln or Asn by PGA leads to a tetrahedral intermediate which breaks down to form an acyl-enzyme intermediate and generates an ammonia molecule as a byproduct. The subsequent hydrolysis of the acyl-enzyme intermediate yields the acidic product and the free enzyme. The conversion of the amide group of the substrate to a carboxylic acid group is proposed to generate electrostatic repulsions causing the flexible loop to change conformation and return back to the open state, thereby releasing the products (Lubkowski et al., 1994). EcA also catalyzes the exchange of oxygen atoms of the β-carboxylic group of aspartic acid with water oxygens. Aspartic acid protonated at the β-carboxylic group is a much better asparaginase substrate than the fully ionized species, and the side chain carboxyl of aspartic acid exhibits a substantially lower acidity when bound to asparaginase (Röhm & Van Etten, 1986).

Initially, PGA was proposed to utilize Thr100 as the attacking nucleophile while a proximal Lys173, which is stabilized by Asp101, would act as a base to augment the nucleophilicity of the catalytic Thr100 residue (Swain et al., 1993; Lubkowski et al., 1994). The same research group also noticed an alternative to this mechanism: Thr20 acting as the attacking nucleophile (Miller et al., 1993). Support for this later hypothesis comes from recently obtained evidence which shows that indeed Thr12 in EcA (and presumably Thr20 in PGA and Thr15 in ErA) can act as the nucleophile (Palm et al., 1996). EcA mutant Thr89Val was allowed to react with asparagine, and a covalent bond between the aspartyl moiety of the substrate and Thr12 was formed. The bond was not hydrolyzed, and the enzyme was trapped as a covalent intermediate. Although this observation does not preclude that in the active native enzyme Thr100 is the actual nucleophile (Palm et al., 1996), it indicates that Thr12 is reactive despite its unremarkable environment. Substrate binding and product release are proposed to be facilitated by the substrate or product interaction with the active site loop which consists of residues Thr20−Gly40 (Lubkowski et al., 1994). The exact nature of the interaction between the active site loop and the substrate or products remains uncertain and should be addressed in greater detail. Lubkowski et al. (1994) reported the structure of PGA with the active site loop in the open conformation at 2.0 Å resolution from type-2 crystals obtained using MPD as the precipitating agent. The reported structure and the corresponding electron density maps did not contain continuous and unambiguous electron density for the active site loop in the closed conformation.

The amino acid sequence of PGA was obtained essentially by chemical sequencing and verified against the electron density maps. Some small regions could not be sequenced and were proposed on the basis of the shape of electron density corresponding to the side chains in Fourier maps (Lubkowski et al., 1994).

We report here the crystal structure of PGA solved at 1.7 Å resolution by the molecular replacement method. The refined structure and resultant electron density maps revealed excellent density for the active site loop in the closed conformation. In addition, electron density for a sulfate ion and most likely an ammonium ion is clearly visible in the active site. Minor revisions to the amino acid sequence for PGA were introduced, and mechanistic implications for the active site loop were examined.

MATERIALS AND METHODS

PGA was purified according to a previously reported method (Roberts, 1976) and stored as a lyophilized powder. Lyophilized PGA was dissolved in ice-cold 10 mM phosphate buffer, pH 7.2, and dialyzed against 10 mM phosphate buffer for a period of 2 days. Crystals of PGA were grown by the hanging drop, vapor diffusion method (McPherson, 1990) with 2.0 M ammonium sulfate as the precipitating reagent. Large diamond-shaped crystals (type-1) with typical dimensions of $2.0 \times 1.5 \times 0.2$ mm^3 began growing after 2 weeks, and crystal growth was apparently complete in 4 weeks. The enzyme crystallizes in space group $C222_1$ with unit cell dimensions $a = 78.62$, $b = 135.80$, and $c = 137.88$ Å. Assuming two protomers per asymmetric unit gave a calculated $V_m = 2.63$ Å^3/Da, which is within the range observed for proteins (Matthews, 1968).

Type-1 PGA crystals grow as very large plates. Mounting them was difficult because the surface tension cracked the crystals when we attempted to dry them. The problem was solved by gently melting 2.0 mm capillaries to provide a flat platform on which the crystals were positioned.

Data Collection and Refinement. The best native data set was collected employing a Rigaku rotating anode source at 50 kV and 100 mA with mirror optics and an R-Axis IV area detector at a distance of 120 mm. After rejection of reflections with $I < 1\sigma(I)$, the data set is 86% complete to 1.7 Å resolution with 68 971 reflections and $R_{merge} = 7.5\%$. Data collection statistics are shown in Table 1. Molecular replacement was used to obtain initial phases using the MERLOT program package. As no crystal structure of PGA

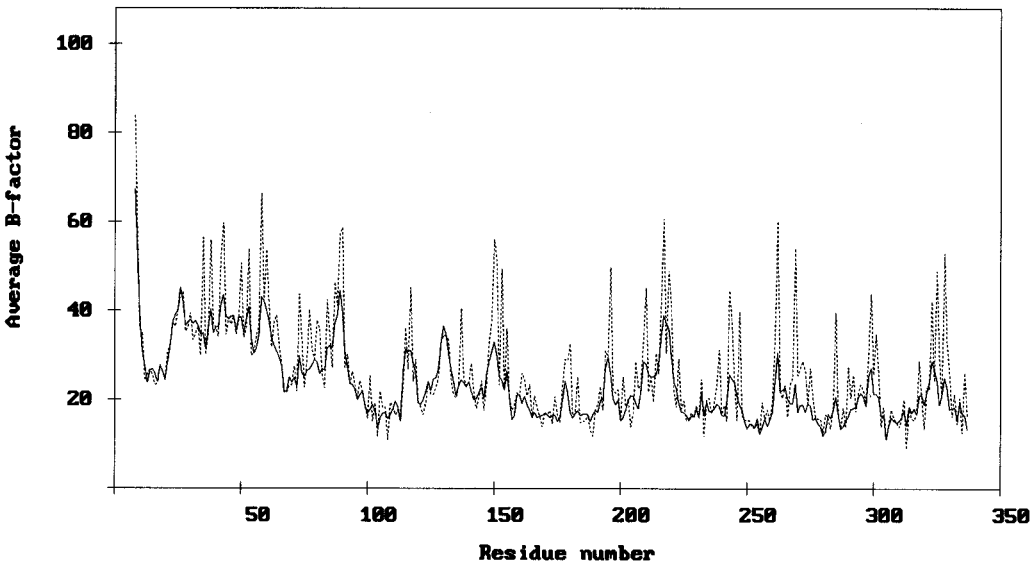

FIGURE 1: Temperature factor plot for subunit A of PGA. The solid lines correspond to average temperature factors of the main chain atoms, and the dashed lines correspond to the average temperature factors of side chain atoms.

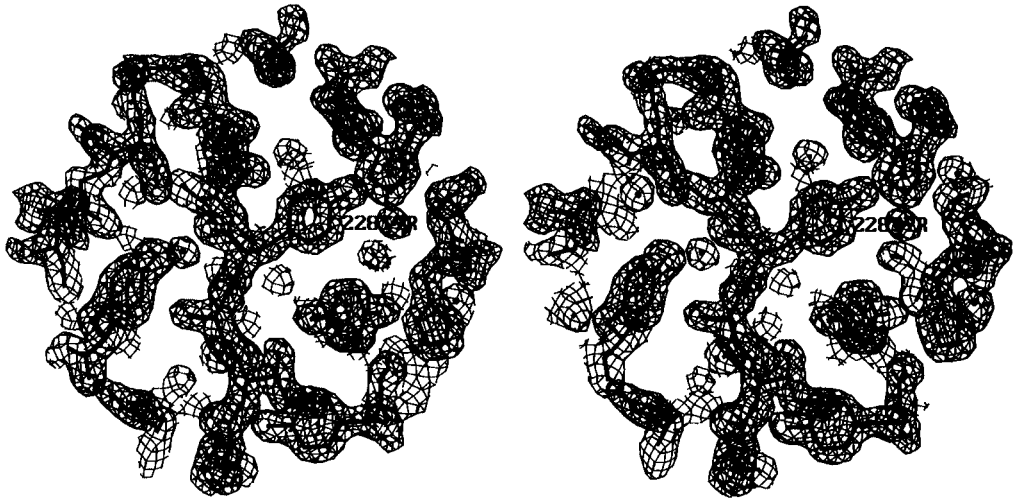

FIGURE 2: Stereoview of a representative portion of the $2F_o - F_c$ electron density map contoured at the 1.5σ level.

was available during the early stages of the structure determination, the following molecular replacement strategy was developed: The amino acid sequence for EcA (Swain et al., 1993) was modified to that of PGA using the program CHAIN. The modified tetramer was then used as the probe model to obtain solutions for the rotational and translational searches and yielded an initial $R = 36.4\%$. The appropriate two subunits were selected for the subsequent refinement. The model was optimized using the simulated annealing option followed by positional and temperature factor refinement with the program package X-PLOR (Brünger, 1992). The positions of the hydrogen atoms from water molecules were set manually to maximize hydrogen bond formation and were not allowed to be repositioned by the generate option of X-PLOR. This reduced subsequent distortion of the water structure by the potential energy term. The final *R*-factor after waters and ligands were added and sequence modifications were made is 19.9% with average deviations from ideal values: bonds, 0.010 Å; angles, 1.2°; dihedrals, 25.8°. Figure 1 shows a plot of the *B*-factors for one of the subunits. The data for the second subunit (not shown) are very similar.

RESULTS

Protomer Structure

The electron density is excellent in general; the positions of almost all atoms are resolved. Also, most side chains with six-membered rings show holes. A representative portion of the $2F_o - F_c$ electron density map is shown in Figure 2. An exception to this well-defined map is seven N-terminal residues for which there is no electron density. Disorder of the same residues was also observed in the other crystal form (Lubkowski et al., 1994). Only a few side chains (mostly lysines) do not have complete electron density; they are listed in Table 2.

Special attention was given to residues 108−118, 264, 266, 269, and 313−321 for which the amino acid sequence was not obtained from chemical sequencing but was based on electron density (Lubkowski et al., 1994). It should be pointed out that the sequence of PGA deposited in the Protein Data Bank (entry 3pga) and SwissProt (P10182) has been revised from that published. In our assessment, all revisions are correct. Analysis of the electron density and hydrogen bonding situation led us to introduce further sequence

Table 2: Side Chains Having Incomplete Density in the Final $2F_o - F_c$ Map Contoured at 1σ Level

residue number, subunit A	disordered atoms	residue number, subunit B	disordered atoms
Lys8	$\gamma, \delta, \epsilon, \zeta$	Lys8	$\gamma, \delta, \epsilon, \zeta$
Gln35	ϵ		
Lys38	ζ	Lys38	δ, ϵ, ζ
Lys43	δ, ϵ, ζ	Lys43	δ, ϵ, ζ
Met137	ϵ	Met137	ϵ
Lys150	$\gamma, \delta, \epsilon, \zeta$	Lys150	δ, ϵ, ζ
		Lys196	δ, ϵ, ζ
Asn210	N_δ		
Gln217	δ, ϵ	Gln217	ϵ_2
Ser219	γ		
		Glu243	δ, ϵ
Lys247	ϵ, ζ	Lys247	ζ
Arg262	$\gamma, \delta, \epsilon, \zeta, \eta$	Arg262	ϵ, ζ, η
Gln269	δ, ϵ	Gln269	γ, δ, ϵ
		Lys272	δ, ϵ, ζ
Lys323	ζ	Lys323	ζ
Lys328	ϵ, ζ	Lys328	δ, ϵ, ζ

Table 3: Proposed Revisions to the Amino Acid Sequence from Protein Data Bank (3pga) and SwissProt (P10182) and the Comparison of the Lubkowski et al. (1994) Published Sequence Against SwissProt (P10182)

residue no.	PDB sequence for 3pga	proposed revisions	residue no.	PDB sequence from SwissProt	PDB sequence from Lubkowski et al. (1994)
111	Asp	Asn	24	A	S
113	Thr	Val	142	N	S
114	Leu	Gln	183	K	L
115	Asn	Lys	205	K	L
263	Leu	Val	223	Q	G
264	Thr	Val	247	K	L
269	Thr	Gln	249	L	I
273	Thr	Asn	266	A	R
317	Val	Ala	311	E	Q
318	Glu	Met	325	Q	N
319	Leu	Val	330	L	I
322	Val	Thr			

modifications, which are listed in Table 3. Figure 3 shows the electron density for the most revised fragment of the protein, residues 317−322.

Over 90% of residues are located in most favored regions of the Ramachandran plot which is shown in Figure 4. The three outliers Ile177, Thr208, and His306 have excellent density with clearly visible carbonyl oxygens. Their deviation from the expected geometry appears to be real and should be attributed to their location on tight turns. Ile177 is the central residue in rarely observed classic γ-turn (Milner-White et al., 1988). The torsion angles ϕ and ψ are close to the values (75°, −64°) ± 40° expected for this type of turn. γ-Turns occur usually at the loop end of a β-hairpin; this turn, however, is located in a larger loop and is followed by a regular β-turn. The second outlier, Thr208, is a part of an overlapping double turn formed by the first turn which includes residues His207−Asn210 followed by the second one which includes residues Thr208−Ser211. Thr208 occupies position $i+1$ in the first turn and simultaneously is a first residue in the second turn. A strong hydrogen bond formed between the Thr208 carbonyl oxygen and the Ser211 nitrogen (N···O = 2.75 Å) is the main reason for the observed deformation. It is worth noticing that on the basis of hydrogen bond patterns most programs like DSSP (Kabsh & Senders, 1983) incorrectly recognize such a double turn as a 3_{10} helix. As this method is routinely used for structures deposited in PDB, it is clear that it may introduce errors in a secondary structure assignment. Also His306 is located in β-turn at position $i+1$. The position of carbonyl oxygen is fixed by two hydrogen bonds: one from the nitrogen atom of Glu289 and one from a water molecule.

The two symmetry independent subunits are very similar. When superposed by least squares the average distance between C_α's is 0.13 Å (rms 0.18 Å); when all atoms are included in the comparison, the average distance is 0.35 Å (rms 0.85 Å). The overall structure is also very similar to the PGA structure reported by Lubkowski et al. (1994); the only significant conformational difference occurs in the region corresponding to the active site loop (Thr20−Gly40). When this region is excluded from the comparisons, the average distance between C_α's is 0.23 Å (rms 0.31 Å); when all atoms are included in the comparison, the average distance is 0.48 Å (rms 0.95 Å). This similarity is an indication that the reported structures are excellent models for the PGA molecule and also that the conformational changes induced by differences in the ionic strength of the mother liquor and crystal packing are very limited. It is unlikely that the solution structure is substantially different from the models.

In the PGA structure reported here, the active site loop is found in the closed conformation, which presumably is present during catalysis. There is excellent electron density for the active site loop in both symmetry independent subunits. Figure 5A shows the electron density for the active site loop of one PGA subunit. Unlike the PGA structure reported by Lubkowski et al. (1994), who described the active site loop as either a bent helix or two separate helices, the loop in the closed conformation does not contain any secondary structural elements. The large conformational rearrangement of the flexible loop is illustrated by the superposition of the open (Lubkowski et al., 1994) and closed PGA structures in Figure 5B. The conformation of PGA's flexible loop is very similar to those found in the catalytic complexes of EcA−aspartate (Swain et al., 1993) and ErA−aspartate (Miller et al., 1993).

SO_4^{2-} and NH_4^+ Coordination

The electron density within the active site is shown in Figure 6, the most dominant feature is a tetrahedral-shaped peak. Since PGA crystals were grown from 2.0 M ammonium sulfate, which inhibits the enzymatic activity of PGA (Roberts, 1976), it is highly likely that the peak corresponds to a sulfate ion. Consequently, a sulfate ion was modeled to fit the density. A neighboring peak, 2.81 Å from O3 of the sulfate ion, forms contacts with the carboxylate oxygens of Asp101 (2.93 Å), Glu68 (2.73 Å), and $Glu_2$294 (3.39 Å), which extends from an adjacent subunit. Such aggregation of anionic groups without a compensating positive charge is unlikely. The distances between the anionic oxygens are much larger than the hydrogen bond distance expected for sharing of a proton which could balance the repulsion; rather they form an approximate tetrahedral arrangement. Therefore we believe that a compensating charge should be attributed to a cation associated with the peak. Since the concentration of ammonium ions is approximately 10^8 that of hydronium ions we believe that this peak corresponds to an ammonium ion (residue 339) rather than a water molecule. The contacts formed by the ammonium ion are shown in

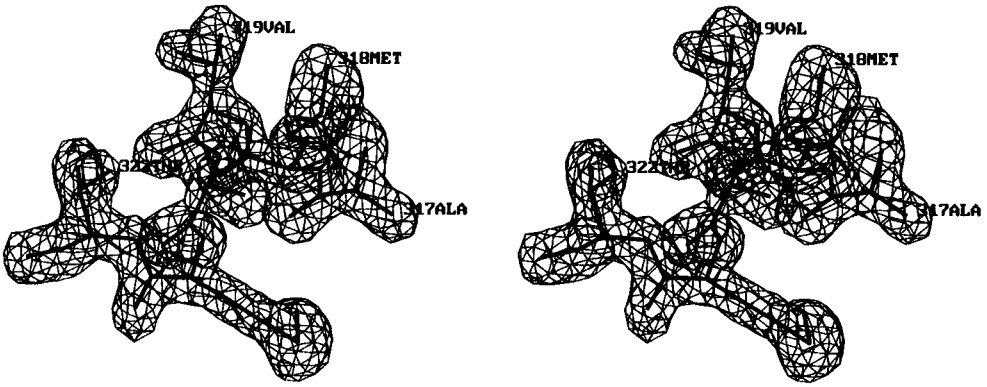

FIGURE 3: Electron density map for residues 317−322 contoured at 1.5σ. It is convincing that 317 = Ala, 318 = Met, 319 = Val, and 322 = Thr.

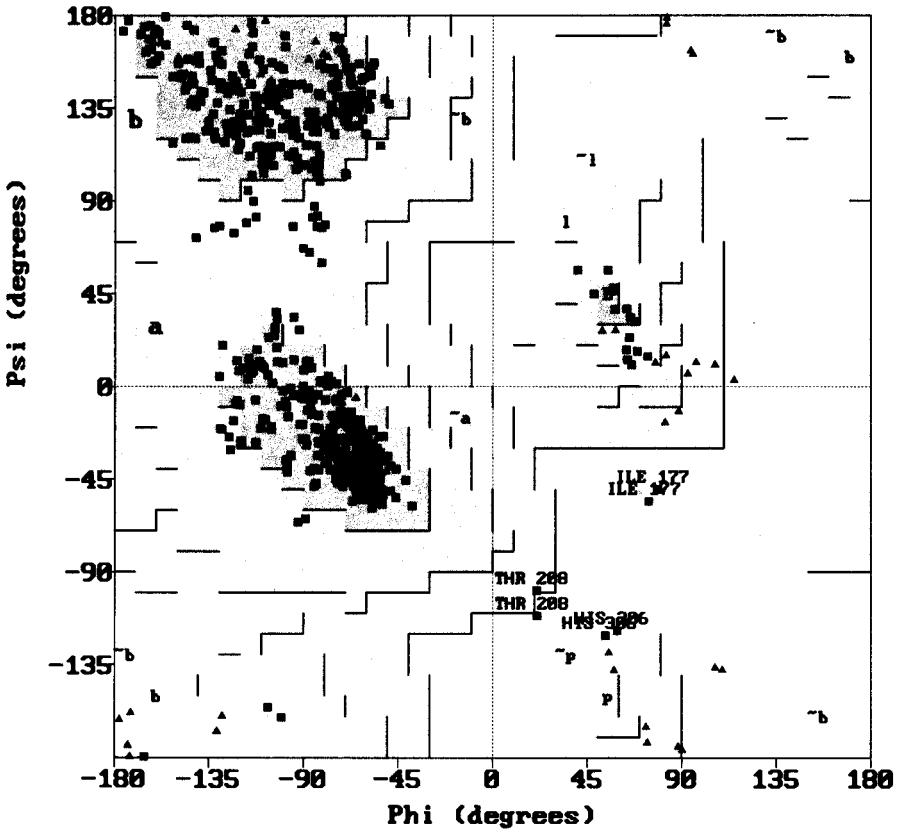

FIGURE 4: Ramachandran diagram showing more than 90% of residues in the most favored regions. Three outliers are noted: Ile177, Thr208, and His306.

Figure 7. Indeed, a superposition of active sites of the ternary inhibitory complex PGA−SO_4^{2-}−NH_4^+ and the catalytic complex EcA−aspartate shows that two oxygen atoms of the sulfate ion closely correspond to the oxygen atoms of the α-carboxylate and a third one to an oxygen atom of the β-carboxylic group. The position of the ammonium ion is 1.25 Å from the α-ammonio group of the aspartic acid zwitterion (Figure 7).

Asp Modeled into Active Site

In order to ascertain further mechanistic information, we modeled an Asp molecule into the active site of closed PGA (Figure 7). The rotation matrix and translation vectors applied to the Asp substrate were obtained from the superposition of EcA and ErA onto closed PGA by least squares fit using the CCP4 program LSQKAB (Kabsch, 1988). Table 4 lists the rotational matrices and translation vectors used for superposition. The PGA active site environment was compared to that of EcA and ErA. Both the positioning and geometry of the catalytic triad and substrate were very similar in all three models (Figure 8). On the basis of hydrogen bonding potentials, we have tentatively assigned OD1 of Asp as the carbonyl oxygen of Asn and the position of OD2 of Asp as the site of amide nitrogen of Asn. OD1 of Asp is the acceptor of two hydrogen bonds: one from the main chain nitrogen of Thr100 at 2.93 Å and the second from the main chain nitrogen of Thr20 at 2.92 Å (Figure 7). Thus, it seems that the flexible loop, upon loop closure, contributes to a possible oxyanion hole necessary for the stabilization of the negatively charged oxygen of the tetrahedral intermediates. OD2 of Asp is located in close proximity to two electronegative atoms: the γ-O of Thr100 (2.62 Å) and the main chain carbonyl oxygen of Ser125 (3.17 Å). Since OD2 of Asp is in close proximity to two hydrogen

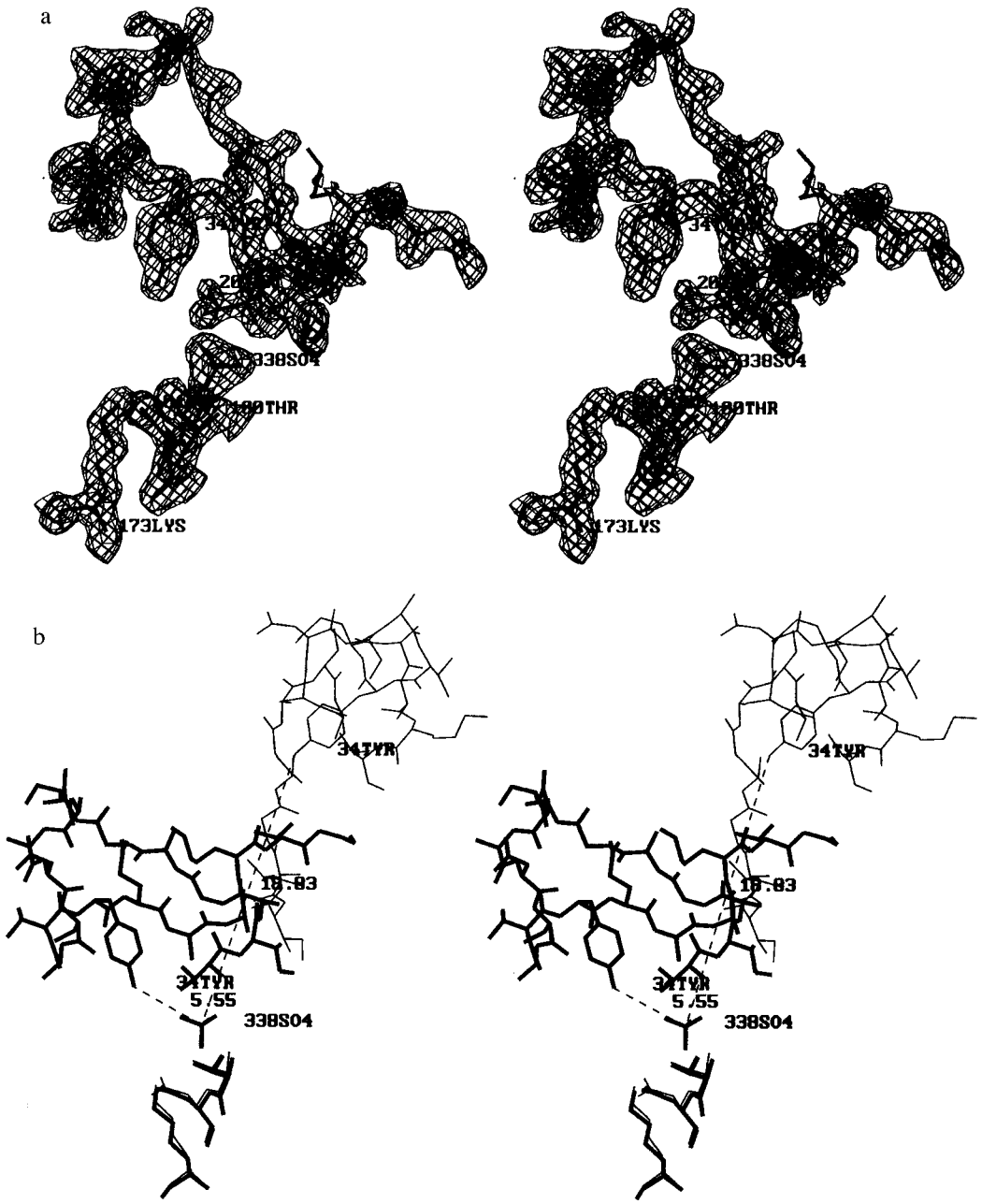

FIGURE 5: (a) $2F_o - F_c$ electron density map for the active site loop of subunit A contoured at 1.5σ. (b) Stereoview of the superposition of the PGA structure in the closed (thick lines) and the open (thin lines) (Lubkowski et al., 1994) conformations illustrating the large rearrangement which takes place upon binding SO_4^{2-} and NH_4^+ ions.

bond acceptors, we believe that the amide nitrogen in this site would be a hydrogen bond donor.

DISCUSSION

The sulfate and ammonium ions provide suitable interactions to stabilize the active site loop in the closed conformation. An analogous situation, cooperative binding of two ions which induces catalytic loop closure, was previously observed in the inhibitory complex enolase−fluoride−phosphate (Lebioda et al., 1993). Thus, it appears that the conformational change of the catalytic loop in asparaginases and enolase is driven predominantly by electrostatic interactions.

The reactivity of the carbonyl group is attributed to the inherent polarity that exists between the carbonyl carbon and the more electronegative oxygen atom. The electrophilic carbonyl carbon is highly susceptible to nucleophilic attack from above or below the plane. Burgi et al. (1974) have studied the most probable routes of attack by the nucleophile. On the basis of experimental and theoretical data, they have shown that an approaching nucleophile, with a distance no greater than 3 Å, lies in a plane bisecting the RCR′ angle. As the distance between the nucleophile and carbonyl carbon decreases, the carbonyl carbon increases its out of plane shift according to a logarithmic relationship. The approach path for typical nucleophilic attack would have the nucleophile approaching along a virtually straight line which is inclined at an angle of approximately 107° relative to the C═O bond and bisects the RCR′ angle. The initial approach geometry of nucleophiles is of crucial importance especially in enzymes where it is controlled by molecular mechanics.

We have superimposed models of three homologous amidohydrolases onto the model of the inhibitory PGA complex utilizing the least squares method as implemented

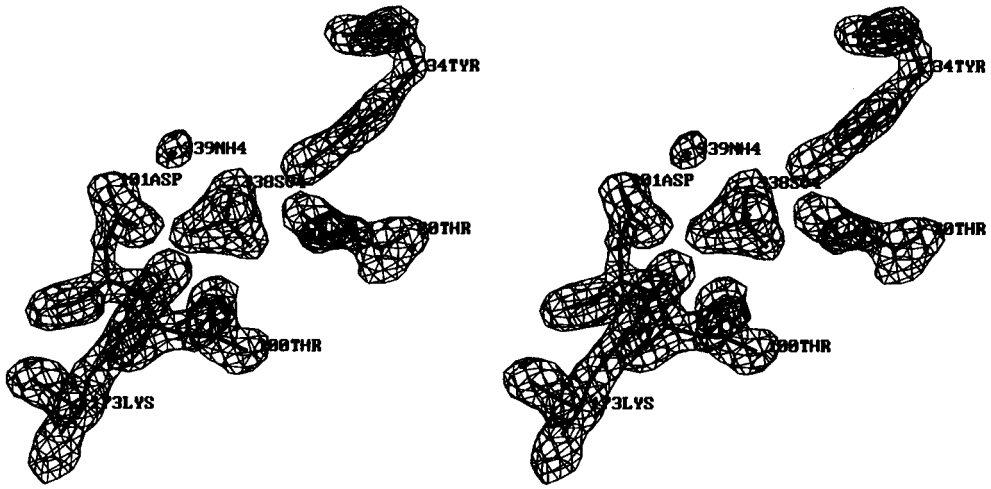

FIGURE 6: $2F_o - F_c$ electron density map of the active site contoured at 1.5σ.

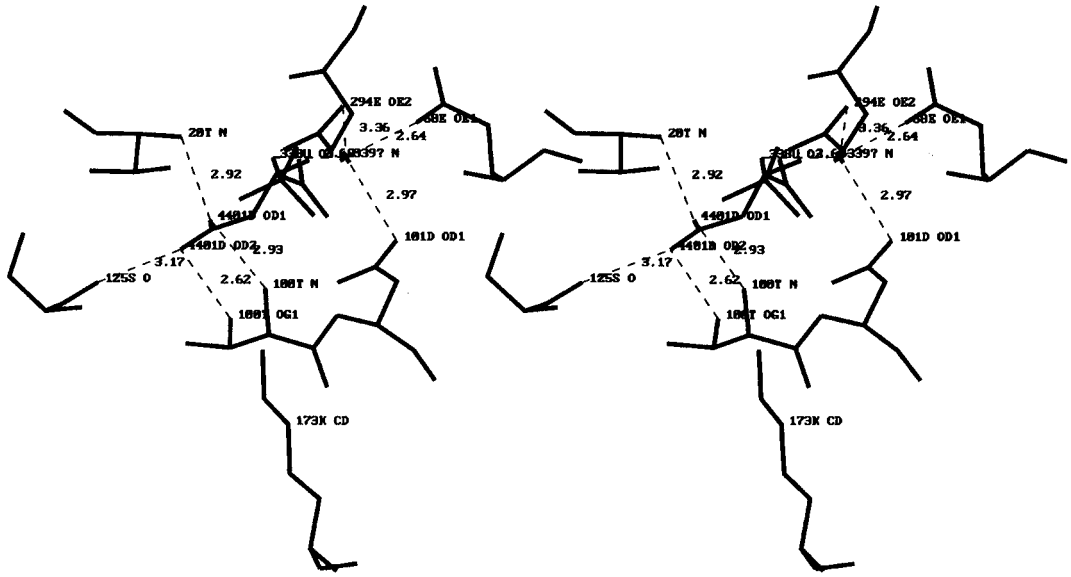

FIGURE 7: Active site of the PGA−SO_4^{2-}−NH_4^+ complex with aspartic acid molecule modeled from the superposition of the ErA−aspartic acid complex onto PGA. Potential hydrogen bonding contacts are shown for the ammonium ion (339) and for the γ-carboxylate oxygens (4401 OD1 and OD2) of the aspartic acid molecule.

Table 4: Superposition of PGA (Lubkowski et al., 1994), ErA (Miller et al., 1993), and EcA (Swain et al., 1993) on the Sulfate−Ammonium−PGA Structure[a]

function	PGA−PGA	ErA−PGA	EcA−PGA
r11	−0.735 69	−0.521 81	−0.151 86
r12	−0.050 45	0.818 24	−0.987 63
r13	−0.675 43	−0.241 23	−0.038 96
r21	−0.062 31	0.829 45	0.493 73
r22	−0.987 95	0.552 73	−0.109 95
r23	0.141 66	0.080 61	0.862 64
r31	−0.674 44	0.199 30	−0.856 25
r32	0.146 30	−0.158 03	0.111 76
r33	0.723 69	−0.967 11	0.504 32
t1	0.969 213	62.046 551	1.117 033
t2	1.345 267	82.829 842	0.638 334
t3	1.193 150	127.245 895	1.214 223
rms (Å)	0.294	0.819	0.872
av displacement (Å)	0.222	0.635	0.711

[a] Rotation matrices and translation vectors were obtained with the LSQKAB (Kabsch, 1988) program.

in LSQKAB (Kabsch, 1988) (Table 4). Two of these models, EcA (Swain et al., 1993) and ErA (Miller et al., 1993), which both contained Asp in the active site, were in the closed conformation. The third model, PGA (Lubkowski et al., 1994), was in the open conformation. The superposition, shown in Figure 8, reveals that a large portion of the active site, which includes the proposed catalytic triad of Thr, Asp, and Lys, does not change its conformation despite different ligands (substrate, ions, or water) present and thus presumably is quite rigid. This is further evidenced by the relatively low temperature factors in these regions (Figure 1).

A crucial aspect of the active site architecture was observed in complexes of EcA and ErA with aspartate. The position of Thr100 in PGA (89 in EcA and 95 in ErA) in relation to the γ-carboxylate group of Asp yields an unfavorable geometry for the nucleophilic addition to the γ-C on the substrate. In order to form a covalent tetrahedral intermediate, the γ-O of Thr100 of PGA (89 of EcA and 95 of ErA) would have to approach γ-C of the substrate. This approach would require a large main chain shift within the active site which is inconsistent with its observed rigidity. In contrast, Thr20 of PGA (12 of EcA and 15 of ErA) located in the active site flexible loop has an excellent geometry to attack the electrophilic γ-C of Asp (Figure 9). Also, the approach

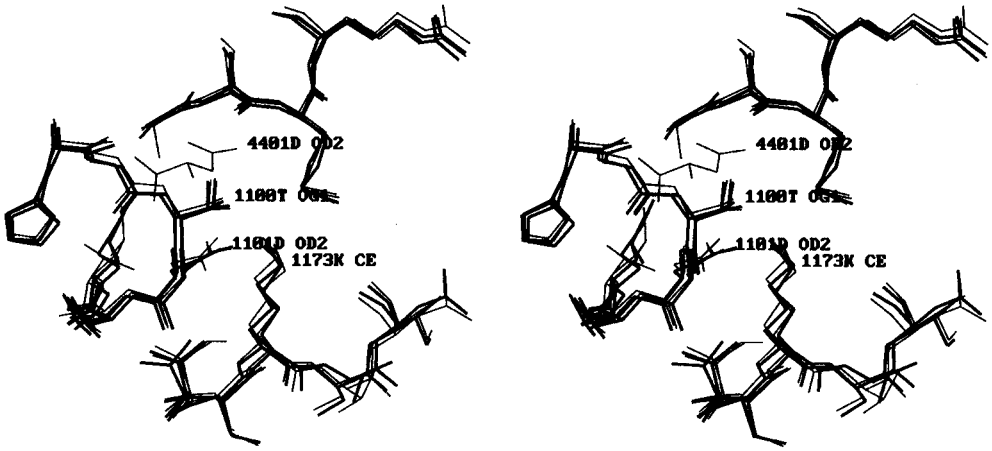

FIGURE 8: Superposition of the main chain atoms of the active sites of native PGA, inhibitory complex PGA$-SO_4^{2-}-NH_4^+$, catalytic complex ErA−Asp, and catalytic complex EcA−Asp. For clarity, only one aspartic acid molecule was included. Different ligands present in the active site do not affect the geometry of the main chain, indicating its rigidity.

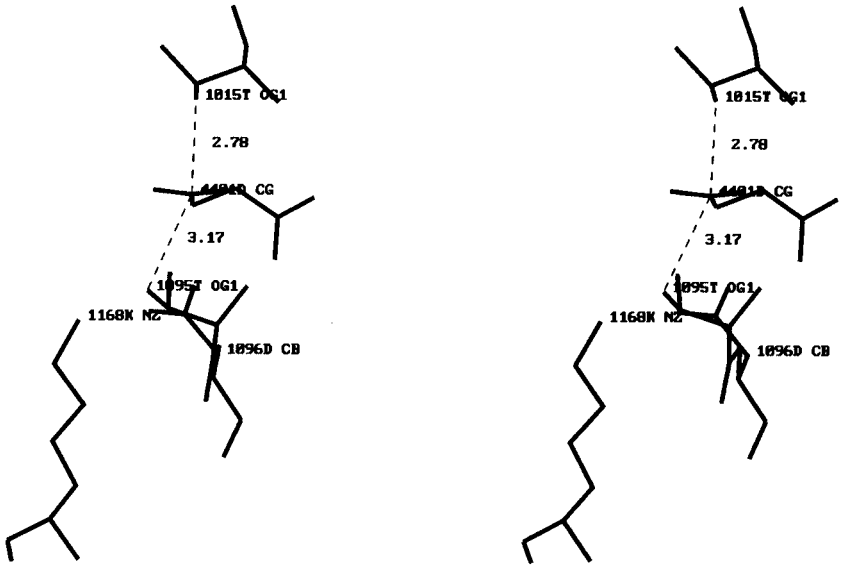

FIGURE 9: Active site of ErA−aspartic acid complex (Miller et al., 1993) showing the positions of the potential catalytic nucleophiles ($Thr15_{ErA}$, $Thr20_{PGA}$ versus $Thr95_{ErA}$, $Thr100_{PGA}$) above and below the plane of the γ-carboxylate group of Asp. The approach of O_γ of $Thr15_{ErA}$ to the C of the substrate can be afforded by a change of the χ_1 torsion angle of the side chain; the approach of O_γ of $Thr95_{ErA}$ requires a movement of the main chain.

and formation of the covalent bond could be afforded by a simple change in the χ_1 torsion angle and perhaps with a small adjustment of the flexible loop. Additional support for Thr20 as the attacking nucleophile comes from site-directed mutagenesis experiments on EcA where Thr12 (20 of PGA and 15 of ErA) was replaced with Ala. The mutation did not affect substrate binding but resulted in activity less than 0.01% of the wild-type enzyme (Harms et al., 1991; Derst et al., 1992). Interestingly, when the glutamine molecule was modeled in the active site with the position of the peptide moiety conserved the hydroxyl of Thr100 appeared to be better positioned for the nucleophilic attack.

The pH profile for PGA shows a broad range (pH 5−10) for glutaminase activity (Roberts, 1976). Röhm and Van Etten (1986) reported a similar pH profile for asparaginase activity by EcA. These studies suggest that in this pH range there is no change in the protonation state of the residues involved in the catalytic mechanism. Lys173, which is in contact with Asp101 and a water molecule, is unlikely to resist protonation in this pH range and be able to serve as the catalytic base. In the absence of substrate, its N_ζ atom has a 10 Å^2 accessible surface.

The absence of any other residue that may accept the proton from either Thr20 or Thr100 suggests that the likely recipient of the proton is the amide nitrogen of the substrate. Such a concept is consistent with the broad pH profile of these enzymes. If the "catalytic triad" is eliminated from the considerations Thr20 (12 of EcA and 15 of ErA) is much better positioned for acting as the nucleophile.

ACKNOWLEDGMENT

We thank Dr. Marzena Miller for the coordinates of ErA.

REFERENCES

Brünger, A. T. (1992) *X-PLOR (Version 3.1) Manual*, Yale University, New Haven, CT.

Burgi, H. B., Dunitz, J. D., Lehn, J. M., & Wipff, G. (1974) *Tetrahedron 30*, 1563−1572.

Citri, N., Kitron, N., & Zyk, N. (1972) *Biochemistry 11*, 2110−2116.

Derst, C., Henseling, J., & Röhm, K. H. (1992) *Protein Eng. 5*, 785−789.

Harms, E., Wehner, A., Aung, H.-P., & Röhm, K. H. (1991) *FEBS Lett. 285*, 55−58.
Kabsch, W. (1988) *J. Appl. Crystallogr. 21*, 916−924.
Kabsch, W., & Sander, C. (1983) *Biopolymers 22*, 2577−2637.
Kidd, J. G. (1970) *Recent Results Cancer Res. 33*, 3−14.
Lebioda, L., Zhang, E., Lewinski, K., & Brewer, J. M. (1993) *Proteins 16*, 219−225.
Lubkowski, J., Wlodawer, A., Ammon, H. L., Copeland, T. D., & Swain, A. L. (1994) *Biochemistry 33*, 10257−10265.
Matthews, B. W. (1968) *J. Mol. Biol. 33*, 491−497.
McGregor, W. G., & Roberts, J. (1989) *Proc. Am. Assoc. Cancer Res. 30*, 2302.
McPherson, A. (1990) *Eur. J. Biochem. 189*, 1−23.
Miller, M., Rao, J. K. M., Wlodawer, A., & Gribskov, M. R. (1993) *FEBS Lett. 328*, 275−279.
Milner-White, E. J., Ross, B. N., Ismail, R., Belhadj-Mostefa, K., & Poet, R. (1988) *J. Mol. Biol. 204*, 777−782.
Montgomery, J. A. (1976) *Prog. Drug Res. 20*, 465−490.
Palm, G. J., Lubkowski, J., Derst, C., Schlepper, S., Röhm, K. H., & Wlodawer, A. (1996) *FEBS Lett. 390*, 211−216.
Roberts, J. (1976) *J. Biol. Chem. 251*, 2119−2123.
Roberts, J., & McGregor, W. G. (1991) *J. Gen. Virol. 72*, 299−305.
Roberts, J., Schmid, F. A., & Rosenfeld, H. J. (1979) *Cancer Treat. Rep. 63*, 1045−1054.
Röhm, K. H., & Van Etten, R. L. (1986) *Arch. Biochem. Biophys. 244*, 128−136.
Swain, A. L., Jaskolski, M., Housset, D., Rao, M., & Wlodawer, A. (1993) *Proc. Natl. Acad. Sci. U.S.A. 90*, 1474−1478.

BI961979X